

Crystallographic Analyses of Isoquinoline Complexes Reveal a New Mode of Metallo- β -Lactamase Inhibition

Guo-Bo Li,^{ab} Jürgen Brem,^{a*} Robert Lesniak,^a Martine I. Abboud,^a Christopher T. Lohans,^a Ian J. Clifton,^a Sheng-Yong Yang,^b Juan-Carlos Jiménez-Castellanos,^c Matthew B. Avison,^c James Spencer,^c Michael A. McDonough,^a and Christopher J. Schofield,^a

CRYSTALLOGRAPHIC ANALYSES OF THE VIM-5 METALLO- β -LACTAMASE (MBL) WITH ISOQUINOLINE INHIBITORS REVEAL NON ZINC ION BINDING MODES. COMPARISON WITH OTHER MBL-INHIBITOR STRUCTURES DIRECTED ADDITION OF A ZINC-BINDING THIOL ENABLING IDENTIFICATION OF POTENT B1 MBL INHIBITORS. THE INHIBITORS POTENTIATE MEROPENEM ACTIVITY AGAINST CLINICAL ISOLATES HARBORING MBLs.

The global spread of antibacterial resistance mediated by metallo- β -lactamases (MBLs), which catalyse hydrolysis of almost all β -lactam antibiotics¹, is an increasing clinical problem.^{2,3} β -Lactamases are divided into classes A, B, C, and D; Class A, C and D use a nucleophilic serine in catalysis, whereas class B MBLs use one or two zinc ions in catalysis (Fig. 1).^{1,4} Serine β -lactamase inhibitors are used clinically in combination with a penicillin or cephalosporin.⁵⁻⁷ No clinically useful MBL inhibitors have been reported, in part because the prevalence of MBL mediated resistance in the clinic has been limited until recently. Most reported MBL inhibitors work via active site metal chelation.^{6,8-13} We are interested in identifying new types of MBL inhibitors¹⁴, which will enable the breadth of activity required for clinical application, whilst not inhibiting structurally related human MBL-fold enzymes^{15,16}. The aim of obtaining the breadth of MBL selectivity is complicated by structural variations in the B1 MBL active site loops, as observed in crystal structures of the Verona Integron-encoded MBL (VIM), Imipenemase (IMP), and New Delhi (NDM) B1 MBLs.¹⁷⁻¹⁹

We recently reported studies comparing the properties of VIM variants.²⁰ The results reveal minor differences in the kinetic parameters of the tested variant/substrate combinations and in the protein folds. However, differences in in-vitro inhibition profiles were observed which may be relevant to inhibitor development. In particular, using a fluorescence-based assay, we observed differences in potencies for enantiomers of tryptophan-isoquinoline linked inhibitors against VIM variants (**1** and **2**, Fig. 2a).²¹ The (*R*)-enantiomer (**1**) was more potent than the (*S*)-enantiomer (**2**) for the tested VIM variants (VIM-5, VIM-2, VIM-4, and VIM-38), whereas the (*R*)-enantiomer (**1**) was selective for VIM-5 and VIM-38 over VIM-1 and VIM-4 (Table S1).²⁰ Both **1** and **2** manifested inhibition (albeit modest) of São Paulo metallo- β -lactamase (SPM)-1, IMP-1, NDM-1, and VIM-2.²¹ Nevertheless isoquinoline based inhibitors show potential for broad-spectrum MBL inhibition. To investigate the mode of action of **1** and **2** against MBLs, we performed crystallographic analyses on VIM-5. The results presented here reveal a new mode of MBL inhibition and enabled the design of modified thiol-based zinc binding compounds leading to more potent inhibitors.

We obtained crystal structures of VIM-5 in complex with **1** and **2** to high resolution; VIM-5:**1** and VIM-5:**2** structures were obtained by co-crystallization (Table S2) and diffracted to 1.96 Å and 1.99 Å resolution, respectively. The VIM-5:**1** structure crystallised with two molecules in the asymmetric unit (space group *P* 2₁ 2₁ 2₁); the VIM-5:**2** structure contains three molecules in the asymmetric unit (space group *F* 2 2 2) (Table S3). In both structures, there was clear $F_o - F_c$ density in the VIM-5 active site, into which **1** and **2** could be confidently modelled (Fig. S1).

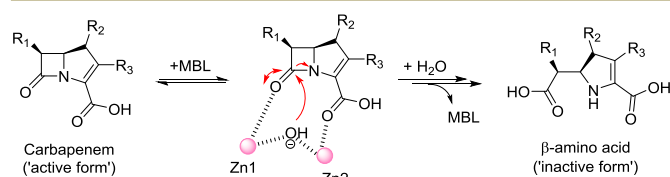


Fig. 1 Outline mechanisms for MBL catalysed β -lactam hydrolysis. Note, in the case of MBLs. Variations of this mechanism are possible dependent on specific enzyme-substrate combinations.

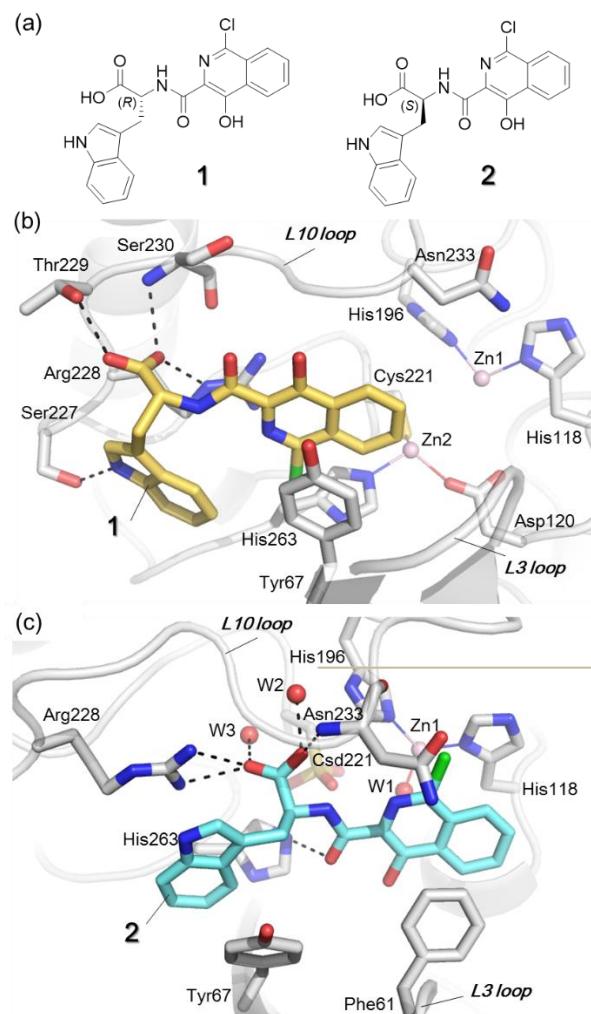


Fig. 2 Binding of inhibitors **1** and **2** to VIM-5. (a) Chemical structures of (*R*)-enantiomer (**1**) and (*S*)-enantiomer (**2**). (b) View of the active site from the VIM-5:1 (PDB ID: 5N58) (c) and VIM-5:2 (PDB ID: 5N55) complexes. Note, in the VIM-5:2 structure, Cys221 is oxidised to a sulphinic acid resulting in loss of one Zn(II) ion.

In the VIM-5:2 structure, oxidation of Cys221 to a sulphinic acid (Csd221) prevented binding of Zn2 (Fig. 2c); we attempted co-crystallization/soaking, but failed to obtain a di-zinc VIM-5 structure in complex with **2**. Crystallisation of this crystal form may have been due to time dependent Cys221 oxidation, since crystals took several weeks to appear under the tested conditions. Superimposition of the mono-zinc VIM-5:2 structure with the di-zinc VIM-5 structure without ligand (PDB ID: 5A87)²⁰ reveals, apart from the different number of bound zinc ions, a similar fold and active site except for small changes in the immediate environment around the oxidised and unoxidised Cys221 (Fig. S3).

We also obtained a structure of VIM-5 in complex with **1** in which Cys221 was oxidised (1.05 Å resolution). This structure revealed a near identical binding mode for **1** as observed in the unoxidised di-zinc VIM-5:1 structure (Fig. S4 and S5). Thus, it appears likely that Cys221 oxidation and loss of one of the two zinc ions from the active site of VIM-5 has a limited effect

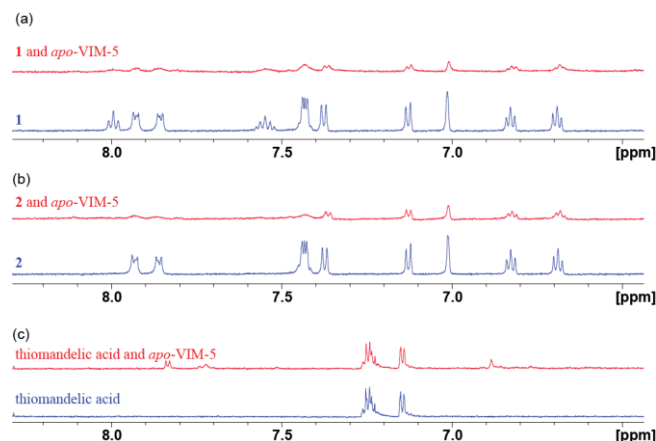


Fig. 3 Binding studies of **1** (a), **2** (b), and thiomandelic acid (c) to *apo*-VIM-5 using CPMG NMR. **1** and **2** bind strongly to *apo*- and di-Zn(II)-VIM-5 as indicated by signal density reduction in the presence of *apo*-VIM-5, while thiomandelic acid only binds very weakly to *apo*-VIM-5, indicating that the active site Zn(II) ions are not essential for binding of **1/2**. Assay mixtures contained 50 μ M *apo*-VIM-5 and 50 μ M of the compound of interest, buffered with 50 mM Tris-D₁₁, pH 7.5, and 0.02 % NaN₃ in 90 % H₂O and 10 % D₂O.

on the binding mode of **1** and, by inference, **2**.

In the VIM-5:**1** complex, **1** binds close, but not directly, to the active site zinc ions and is positioned to interact with the catalytically important residues Arg228 and Tyr67 (using standard BBL MBL numbering²²) (Fig. 2b). The carboxylate of **1** is positioned to make hydrogen-bond and electrostatic interactions with Ser227, Arg228, Thr229, and Ser230 on the L10 loop, and its isoquinoline ring is positioned to π - π stack with Tyr67 on the L3 loop and make cation- π interactions with Arg228 (Fig. 2b and Fig. S2a). Similarly to the binding of **1**, **2** binds adjacent to, but not directly with, the active site zinc ions (Fig. 2c); its carboxylate positioned to form hydrogen bonds with Arg228 and Asn233 on the L10 loop (similar to the carboxylate of β -lactam substrates), and its isoquinoline and indole moieties are positioned to make π - π stacking interactions with Phe61 and Try67 on the L3 loop, respectively (Fig. 2c and Fig. S2b).

The crystallographic analyses of **1** and **2** with VIM-5 thus reveal an inhibition mode that does not involve direct zinc chelation. To validate this mode, we used ¹H Carr-Purcell-Meiboom-Gill (CPMG) and ligand-observe NMR (water-ligand observed gradient spectroscopy, wLOGSY) to test for binding to di-Zn(II) and *apo*-VIM-5.¹⁴ The latter was catalytically inert and generated by incubation of di-Zn(II)-VIM-5 with ethylenediaminetetraacetic acid (EDTA) (Fig. S6). The results reveal **1** and **2** bind strongly to both *apo*-VIM-5 (Fig. 3a-b, S7a-b) and di-Zn(II)-VIM-5 (K_D values for **1** and **2**, 0.8 μ M and 1.03 μ M, respectively, (using racemic thiomandelic acid as a reporter molecule Fig. S9a-b)²⁰). In contrast, thiomandelic acid, a broad-spectrum MBL inhibitor²³, does not bind to *apo*-VIM-5 (Fig. 3c, S7c, S8); K_D for thiomandelic acid with di-Zn(II)-VIM-5, 170 nM (Fig. S9c). Thus, zinc ions are not required for **1** and **2** to bind to VIM-5 in solution, consistent with the binding mode observed in the crystal structures.

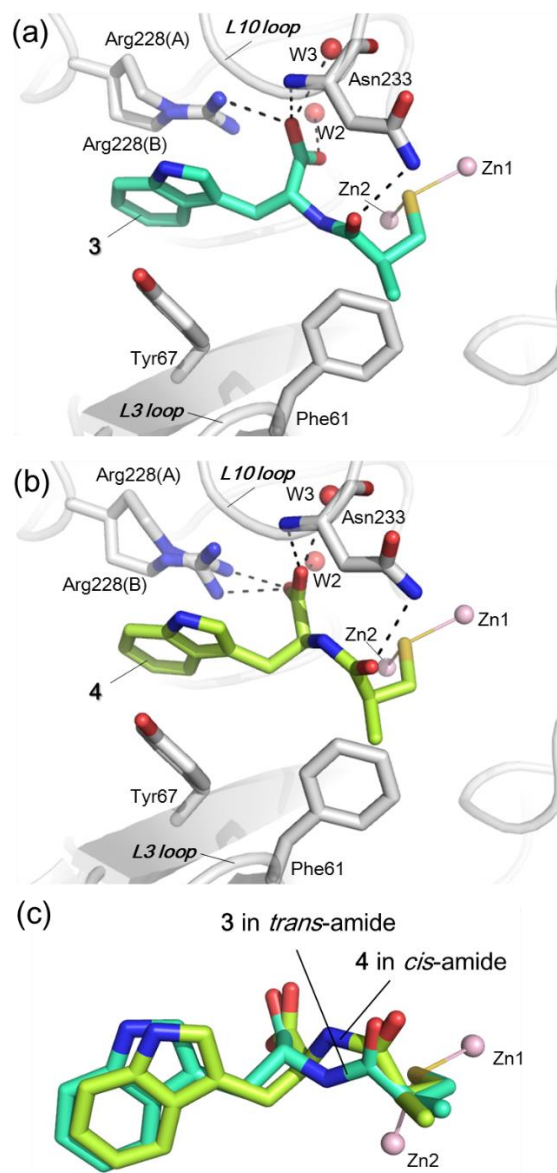


Fig. 4 Crystallographic analyses reveal **3** and **4** bind to the VIM-2 MBL via similar modes. (a) View from a structure of **3** complexed with VIM-2 (PDB ID: 5N4S). (b) View from a structure of **4** complexed with VIM-2 (PDB ID: 5N4T). (c) Superimposition of VIM-2:**3** and VIM-2:**4** reveals **3** and **4** bind in similar modes involving zinc chelation. Note that unlike **3**, **4** is bound with *cis*-amide conformation.

Comparison of VIM-5:1 and VIM-5:2 structures with reported MBL-inhibitor complexes, reveals the carboxylate of **2** binds similarly to that of D-/L-captopril (Fig. S10),¹⁷ i.e. via electrostatic interactions with Arg228 in VIM-2 and VIM-5, or equivalent residue, Lys224 in IMP-1 and BclI, which are also bind the β -lactam antibiotic carboxylate (Fig. S11).^{9, 17} Based on these structures we designed and synthesized two compounds (**3** and **4**, Table 1) that combine the tryptophan moiety of **2** and the (*S*)-3-mercapto-2-methylpropanal moiety of D-/L-captopril (Supplementary Methods Scheme S1 for **3/4** synthesis), with the aim of identifying broad-spectrum MBL inhibitors.

3 and **4** displayed the most potent inhibition to VIM-2 MBL (Table 1). To investigate their binding modes, we obtained structures of VIM-2 in complex with **3** then to 1.20 and 1.16 Å resolution, respectively (Table S3). As predicted, the structures reveal that the thiol of **3** and **4** chelates to and bridges the two zinc ions, as observed for captopril¹⁷ and related thiol based inhibitors^{24, 25} (Fig. 4a-b, S12, S13); as observed for **2**, **3** and **4** are positioned to form electrostatic interactions with Arg228 and Asn233, and hydrophobic interactions with Phe61 and Tyr67 (Fig. 4a-b, S13, S14). Notably, **3** and **4**, like **2**, bind in a mode similar to hydrolysed β -lactam product (Fig. S15). Notably, in the VIM-2:**4** structure, the amido group adopts a *cis*-conformation (Fig. 4c). By contrast, the *trans*-conformation is observed in the VIM-2:**3** structure, where the amido group of **3** binds very similar to that of D-captopril (Fig. S16). These differences may, in part, explain why **3** is more potent against VIM-2 than **4**; superimposing structures of VIM-2:**3** and VIM-2:**4** with VIM-5:2 reveals that these compounds bind *via* a similar binding mode (Fig. S14).

3 and **4** manifest broad-spectrum inhibition against the class B MBLs (clinically relevant subclass B1 enzymes VIM-2, VIM-1, VIM-5, IMP-1, NDM-1, SPM-1, and BclI, the subclass B2 enzyme CphA, and the subclass B3 enzyme L1^{21, 26, 27}), and are more

potent than D- or L-captopril (Table 1); **3**, with nanomolar potency for subclass B1 MBLs (IMP-1, VIM-2, VIM-1, VIM-5 and SPM-1), is relatively more potent than **4**. As **1** and **2** occupy slightly different regions of the VIM-5 active site (Fig 2b, 2c, and S17), we synthesized **5** that merges the indole moiety of **1** and the isoquinoline of **2** via a linker (Supplementary Methods Scheme S2). However, **5** only showed weak inhibition against VIM-5 (IC₅₀, 41 μM).

Since derivatives of **3** and **4** may have clinical prospects due to their synthesis tractability and potent inhibition against subclass B1 MBLs, we tested them against a panel of MBL-producing derivatives of three clinically important multidrug-resistant species: *Escherichia coli*, *Enterobacter aerogenes* and *Klebsiella pneumoniae*. The minimum inhibitory concentrations (MICs) of meropenem against the bacterial strains were determined with and without MBL inhibitors. **3** and **4** potentiated the efficacy of meropenem against VIM-1 and IMP-1-producing strains, with **3** conferring clinically-relevant meropenem susceptibility (MIC < 8 mg/L) in all cases when used at 50 μM (Table 2).

In conclusion, crystallographic analyses of the clinically relevant VIM-5 B1 MBL in complex with enantiomeric isoquinolines **1** and **2** reveal that although they interact with slightly different regions of the VIM-5 active site (Fig. 2), binding of each involves catalytically important residues on the catalytically important L3 and L10 loops.^{14, 28} The combined crystallographic and solution results also reveal an MBL inhibition mode not involving Zn(II) ion chelation. Comparison of VIM-5:**1** and VIM-5:**2** structures with recently reported inhibitor-MBL structures led to the design of highly potent, broad-spectrum MBL inhibitors **3** and **4**. **3** and **4** were also found to potentiate the efficacy of meropenem against MBL-producing strains. Since **3** and **4** can be readily prepared, they are good starting points for further optimisation.

Table 1. IC₅₀ values (μM) of **3**, **4**, D-captopril and L-captopril against clinically relevant MBLs.

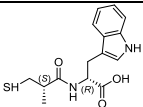
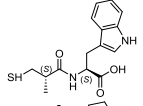
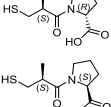
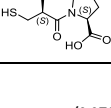
ID	Chemical Structure	Class B1						B2		B3
		VIM5	VIM2	VIM1	NDM-1	SPM-1	BcII	IMP-1	CphA	L1
3		0.175	0.055	0.526	24.81	0.890	1.63	0.041	~400	16.21
4		2.187	1.06	33.73	64.8	0.260	30.4	3.98	>400	97.3
D-captopril		14.9	4.54	7.452	62.1	1.156	12.03	6.75	>400	67.08
L-captopril		10.5	2.47	42.84	196.8	1.654	47.82	2.50	>400	73.73

Table 2. MICs of meropenem (MEM) with and without **3** and **4** against MBL-producing bacteria.

Strain	MEM MIC (mg/liter)						
	DMSO	3 (10μM)	3 (25μM)	3 (50μM)	4 (10μM)	4 (25μM)	4 (50μM)
<i>E. coli</i> + IMP-1	32	32	8	0.5	32	32	32
<i>Ent. aerogenes</i> + IMP-1	32	16	0.5	0.5	32	16	8
<i>K. pneumoniae</i> + IMP-1	32	8	1	0.125	32	8	8
<i>E. coli</i> + VIM-1	16	8	4	0.25	16	16	8
<i>Ent. aerogenes</i> + VIM-1	16	8	8	0.5	16	16	16
<i>K. pneumoniae</i> + VIM-1	16	16	4	0.5	16	16	16

We thank the staff at the Diamond Synchrotron Light source for access, and Dr Aisha Al-Amri and Mohammed Alorabi who, respectively, made the blaIMP-1 and blaVIM-1 plasmids. This work was supported by the Wellcome Trust, the Medical Research Council (MRC) grant MR/L007665/1, the Medical Research Council (MRC)/Canadian Grant G1100135, the SWON alliance (C. J. Schofield), the National Natural Science Foundation of China (81502989) (G.-B. Li), and National Institute of Allergy and Infectious Diseases of the U.S. National Institutes of Health R01AI100560 (J. Spencer).

Notes and references

- K. Bush and G. A. Jacoby, *Antimicrob. Agents Chemother.*, 2010, **54**, 969.
- G. Cornaglia, H. Giamarellou and G. M. Rossolini, *Lancet Infect. Dis.*, 2011, **11**, 381.
- M. F. Mojica, R. A. Bonomo and W. Fast, *Curr. Drug Targets*, 2016, **17**, 1029.
- M. W. Crowder, J. Spencer and A. J. Vila, *Acc. Chem. Res.*, 2006, **39**, 721.
- A. R. White, C. Kaye, J. Poupard, R. Pypstra, G. Woodnutt and B. Wynne, *J. Antimicrob. Chemother.*, 2004, **53**, i3.
- S. M. Drawz and R. A. Bonomo, *Clin. Microbiol. Rev.*, 2010, **23**, 160.
- D. Y. Wang, M. I. Abboud, M. S. Markoulides, J. Brem and C. J. Schofield, *Future Med. Chem.*, 2016, **8**, 1063.
- J. Brem, S. S. van Berkel, W. Aik, A. M. Rydzik, M. B. Avison, I. Pettinati, K.-D. Umland, A. Kawamura, J. Spencer, T. D. Claridge, M. A. McDonough and C. J. Schofield, *Nat. Chem.*, 2014, **6**, 1084.
- P. Hinchliffe, M. M. Gonzalez, M. F. Mojica, J. M. Gonzalez, V. Castillo, C. Saiz, M. Kosmopoulou, C. L. Tooke, L. I. Llarrull, G. Mahler, R. A. Bonomo, A. J. Vila and J. Spencer, *Proc. Natl. Acad. Sci. U.S.A.*, 2016, **113**, E3745.

- 10 J. Brem, R. Cain, S. Cahill, M. A. McDonough, I. J. Clifton, J.-C. Jimenez-Castellanos, M. B. Avison, J. Spencer, C. W. G. Fishwick and C. J. Schofield, *Nat. Commun.*, 2016, **7**.
- 11 T. Christopeit, T. J. O. Carlsen, R. Helland and H.-K. S. Leiros, *J. Med. Chem.*, 2015, **58**, 8671.
- 12 M. I. Abboud, P. Hinchliffe, J. Brem, R. Macsics, I. Pfeffer, A. Makena, K.-D. Umland, A. M. Rydzik, G.-B. Li, J. Spencer, T. D. W. Claridge and C. J. Schofield, *Angew. Chem. Int. Edit.*, 2017, **56**, 3862.
- 13 M. I. Abboud, C. Damblon, J. Brem, N. Smargiasso, P. Mercuri, B. Gilbert, A. M. Rydzik, T. D. W. Claridge, C. J. Schofield and J.-M. Frère, *Antimicrob. Agents Chemother.*, 2016, **60**, 5655.
- 14 G.-B. Li, M. I. Abboud, J. Brem, H. Someya, C. T. Lohans, S.-Y. Yang, J. Spencer, D. W. Wareham, M. A. McDonough and C. J. Schofield, *Chem. Sci.*, 2017, **8**, 928.
- 15 I. Pettinati, J. Brem, S. Y. Lee, P. J. McHugh and C. J. Schofield, *Trends Biochem. Sci.*, 2016, **41**, 338.
- 16 S. Y. Lee, J. Brem, I. Pettinati, T. D. Claridge, O. Gileadi, C. J. Schofield and P. J. McHugh, *Chem. Commun.*, 2016, **52**, 6727.
- 17 J. Brem, S. S. van Berkel, D. Zollman, S. Y. Lee, O. Gileadi, P. J. McHugh, T. R. Walsh, M. A. McDonough and C. J. Schofield, *Antimicrob. Agents Chemother.*, 2016, **60**, 142.
- 18 J.-F. Wang and K.-C. Chou, *Curr. Top. Med. Chem.*, 2013, **13**, 1242.
- 19 P. W. Groundwater, S. Xu, F. Lai, L. Váradi, J. Tan, J. D. Perry and D. E. Hibbs, *Future Med. Chem.*, 2016, **8**, 993.
- 20 A. Makena, A. Ö. Düzgün, J. Brem, M. A. McDonough, A. M. Rydzik, M. I. Abboud, A. Saral, A. Ç. Çiçek, C. Sandalli and C. J. Schofield, *Antimicrob. Agents Chemother.*, 2016, **60**, 1377.
- 21 S. S. van Berkel, J. Brem, A. M. Rydzik, R. Salimraj, R. Cain, A. Verma, R. J. Owens, C. W. Fishwick, J. Spencer and C. J. Schofield, *J. Med. Chem.*, 2013, **56**, 6945.
- 22 M. Galleni, J. Lamottebrasseur, G. M. Rossolini, J. Spencer, O. Dideberg and J. Frere, *Antimicrob. Agents Chemother.*, 2001, **45**, 660.
- 23 A. I. Karsisiotis, C. F. Damblon and G. C. Roberts, *Biochem. J.*, 2013, **456**, 397.
- 24 O. K. Arjomandi, W. M. Hussein, P. Vella, Y. Yusof, H. E. Sidjabat, G. Schenk and R. P. McGeary, *Eur. J. Med. Chem.*, 2016, **114**, 318.
- 25 B. M. R. Lienard, G. Garau, L. Horsfall, A. I. Karsisiotis, C. Damblon, P. Lassaux, C. Papamicael, G. C. K. Roberts, M. Galleni, O. Dideberg, J.-M. Frere and C. J. Schofield, *Org. Biomol. Chem.*, 2008, **6**, 2282.
- 26 L. Nauton, R. Kahn, G. Garau, J.-F. Hernandez and O. Dideberg, *J. Mol. Biol.*, 2008, **375**, 257.
- 27 L. Horsfall, G. Garau, B. Liénard, O. Dideberg, C. Schofield, J. Frere and M. Galleni, *Antimicrob. Agents Chemother.*, 2007, **51**, 2136.
- 28 J. Brem, W. B. Struwe, A. M. Rydzik, H. Tarhonskaya, I. Pfeffer, E. Flashman, S. S. van Berkel, J. Spencer, T. D. Claridge, M. A. McDonough, J. L. Benesch and C. J. Schofield, *Chem. Sci.*, 2015, **6**, 956.